

Search for Anomalous Heavy-Flavor Quark Production in Association with W Bosons

- V. M. Abazov,³⁴ B. Abbott,⁷¹ M. Abolins,⁶² B. S. Acharya,²⁸ M. Adams,⁴⁹ T. Adams,⁴⁷ M. Agelou,¹⁷ J.-L. Agram,¹⁸ S. H. Ahn,³⁰ M. Ahsan,⁵⁶ G. D. Alexeev,³⁴ G. Alkhazov,³⁸ A. Alton,⁶¹ G. Alverson,⁶⁰ G. A. Alves,² M. Anastasoaie,³³ T. Andeen,⁵¹ S. Anderson,⁴³ B. Andrieu,¹⁶ Y. Arnoud,¹³ A. Askew,⁷⁵ B. Åsman,³⁹ O. Atramontov,⁵⁴ C. Autermann,²⁰ C. Avila,⁷ F. Badaud,¹² A. Baden,⁵⁸ B. Baldin,⁴⁸ P. W. Balm,³² S. Banerjee,²⁸ E. Barberis,⁶⁰ P. Bargassa,⁷⁵ P. Baringer,⁵⁵ C. Barnes,⁴¹ J. Barreto,² J. F. Bartlett,⁴⁸ U. Bassler,¹⁶ D. Bauer,⁵² A. Bean,⁵⁵ S. Beauceron,¹⁶ M. Begel,⁶⁷ A. Bellavance,⁶⁴ S. B. Beri,²⁶ G. Bernardi,¹⁶ R. Bernhard,^{48,*} I. Bertram,⁴⁰ M. Besançon,¹⁷ R. Beuselinck,⁴¹ V. A. Bezzubov,³⁷ P. C. Bhat,⁴⁸ V. Bhatnagar,²⁶ M. Binder,²⁴ C. Biscarat,⁴⁰ K. M. Black,⁵⁹ I. Blackler,⁴¹ G. Blazey,⁵⁰ F. Blekman,³² S. Blessing,⁴⁷ D. Bloch,¹⁸ U. Blumenschein,²² A. Boehnlein,⁴⁸ O. Boeriu,⁵³ T. A. Bolton,⁵⁶ F. Borcherding,⁴⁸ G. Borissov,⁴⁰ K. Bos,³² T. Bose,⁶⁶ A. Brandt,⁷³ R. Brock,⁶² G. Brooijmans,⁶⁶ A. Bross,⁴⁸ N. J. Buchanan,⁴⁷ D. Buchholz,⁵¹ M. Buehler,⁴⁹ V. Buescher,²² S. Burdin,⁴⁸ T. H. Burnett,⁷⁷ E. Busato,¹⁶ J. M. Butler,⁵⁹ J. Bystricky,¹⁷ W. Carvalho,³ B. C. K. Casey,⁷² N. M. Cason,⁵³ H. Castilla-Valdez,³¹ S. Chakrabarti,²⁸ D. Chakraborty,⁵⁰ K. M. Chan,⁶⁷ A. Chandra,²⁸ D. Chapin,⁷² F. Charles,¹⁸ E. Cheu,⁴³ L. Chevalier,¹⁷ D. K. Cho,⁶⁷ S. Choi,⁴⁶ B. Choudhary,²⁷ T. Christiansen,²⁴ L. Christofek,⁵⁵ D. Claes,⁶⁴ B. Clément,¹⁸ C. Clément,³⁹ Y. Coadou,⁵ M. Cooke,⁷⁵ W. E. Cooper,⁴⁸ D. Coppage,⁵⁵ M. Corcoran,⁷⁵ A. Cothenet,¹⁴ M.-C. Cousinou,¹⁴ B. Cox,⁴² S. Crépé-Renaudin,¹³ M. Cristeti,⁴⁶ D. Cutts,⁷² H. da Motta,² B. Davies,⁴⁰ G. Davies,⁴¹ G. A. Davis,⁵¹ K. De,⁷³ P. de Jong,³² S. J. de Jong,³³ E. De La Cruz-Burelo,³¹ C. De Oliveira Martins,³ S. Dean,⁴² F. Déliot,¹⁷ M. Demarteau,⁴⁸ R. Demina,⁶⁷ P. Demine,¹⁷ D. Denisov,⁴⁸ S. P. Denisov,³⁷ S. Desai,⁶⁸ H. T. Diehl,⁴⁸ M. Diesburg,⁴⁸ M. Doidge,⁴⁰ H. Dong,⁶⁸ S. Doulas,⁶⁰ L. V. Dudko,³⁶ L. Duflot,¹⁵ S. R. Dugad,²⁸ A. Duperrin,¹⁴ J. Dyer,⁶² A. Dyshkant,⁵⁰ M. Eads,⁵⁰ D. Edmunds,⁶² T. Edwards,⁴² J. Ellison,⁴⁶ J. Elmsheuser,²⁴ J. T. Eltzroth,⁷³ V. D. Elvira,⁴⁸ S. Eno,⁵⁸ P. Ermolov,³⁶ O. V. Eroshin,³⁷ J. Estrada,⁴⁸ D. Evans,⁴¹ H. Evans,⁶⁶ A. Evdokimov,³⁵ V. N. Evdokimov,³⁷ J. Fast,⁴⁸ S. N. Fataki,⁵⁹ L. Feligioni,⁵⁹ T. Ferbel,⁶⁷ F. Fiedler,²⁴ F. Filthaut,³³ W. Fisher,⁶⁵ H. E. Fisk,⁴⁸ M. Fortner,⁵⁰ H. Fox,²² W. Freeman,⁴⁸ S. Fu,⁴⁸ S. Fuess,⁴⁸ T. Gadfort,⁷⁷ C. F. Galea,³³ E. Gallas,⁴⁸ E. Galyaev,⁵³ C. Garcia,⁶⁷ A. Garcia-Bellido,⁷⁷ J. Gardner,⁵⁵ V. Gavrilov,³⁵ P. Gay,¹² D. Gelé,¹⁸ R. Gelhaus,⁴⁶ K. Genser,⁴⁸ C. E. Gerber,⁴⁹ Y. Gershtein,⁷² G. Ginther,⁶⁷ T. Golling,²¹ B. Gómez,⁷ K. Gounder,⁴⁸ A. Goussiou,⁵³ P. D. Grannis,⁶⁸ S. Greder,¹⁸ H. Greenlee,⁴⁸ Z. D. Greenwood,⁵⁷ E. M. Gregores,⁴ Ph. Gris,¹² J.-F. Grivaz,¹⁵ L. Groer,⁶⁶ S. Grünendahl,⁴⁸ M. W. Grünewald,²⁹ S. N. Gurzhiev,³⁷ G. Gutierrez,⁴⁸ P. Gutierrez,⁷¹ A. Haas,⁶⁶ N. J. Hadley,⁵⁸ S. Hagopian,⁴⁷ I. Hall,⁷¹ R. E. Hall,⁴⁵ C. Han,⁶¹ L. Han,⁴² K. Hanagaki,⁴⁸ K. Harder,⁵⁶ R. Harrington,⁶⁰ J. M. Hauptman,⁵⁴ R. Hauser,⁶² J. Hays,⁵¹ T. Hebbeker,²⁰ D. Hedin,⁵⁰ J. M. Heinmiller,⁴⁹ A. P. Heinson,⁴⁶ U. Heintz,⁵⁹ C. Hensel,⁵⁵ G. Hesketh,⁶⁰ M. D. Hildreth,⁵³ R. Hirosky,⁷⁶ J. D. Hobbs,⁶⁸ B. Hoeneisen,¹¹ M. Hohlfeld,²³ S. J. Hong,³⁰ R. Hooper,⁷² P. Houben,³² Y. Hu,⁶⁸ J. Huang,⁵² I. Iashvili,⁴⁶ R. Illingworth,⁴⁸ A. S. Ito,⁴⁸ S. Jabeen,⁵⁵ M. Jaffré,¹⁵ S. Jain,⁷¹ V. Jain,⁶⁹ K. Jakobs,²² A. Jenkins,⁴¹ R. Jesik,⁴¹ K. Johns,⁴³ M. Johnson,⁴⁸ A. Jonckheere,⁴⁸ P. Jonsson,⁴¹ H. Jöstlein,⁴⁸ A. Juste,⁴⁸ D. Käfer,²⁰ W. Kahl,⁵⁶ S. Kahn,⁶⁹ E. Kajfasz,¹⁴ A. M. Kalinin,³⁴ J. Kalk,⁶² D. Karmanov,³⁶ J. Kasper,⁵⁹ D. Kau,⁴⁷ R. Kaur,²⁶ R. Kehoe,⁷⁴ S. Kermiche,¹⁴ S. Kesisoglou,⁷² A. Khanov,⁶⁷ A. Kharchilava,⁵³ Y. M. Kharzeev,³⁴ K. H. Kim,³⁰ B. Klma,⁴⁸ M. Klute,²¹ J. M. Kohli,²⁶ M. Kopal,⁷¹ V. M. Korablev,³⁷ J. Kotcher,⁶⁹ B. Kothari,⁶⁶ A. Koubarovsky,³⁶ A. V. Kozelov,³⁷ J. Kozminski,⁶² S. Krzywdzinski,⁴⁸ S. Kuleshov,³⁵ Y. Kulik,⁴⁸ A. Kumar,²⁷ S. Kunori,⁵⁸ A. Kupco,¹⁰ T. Kurča,¹⁹ S. Lager,³⁹ N. Lahrichi,¹⁷ G. Landsberg,⁷² J. Lazoflores,⁴⁷ A.-C. Le Bihan,¹⁸ P. Lebrun,¹⁹ S. W. Lee,³⁰ W. M. Lee,⁴⁷ A. Leflat,³⁶ F. Lehner,^{48,*} C. Leonidopoulos,⁶⁶ P. Lewis,⁴¹ J. Li,⁷³ Q. Z. Li,⁴⁸ J. G. R. Lima,⁵⁰ D. Lincoln,⁴⁸ S. L. Linn,⁴⁷ J. Linnemann,⁶² V. V. Lipaev,³⁷ R. Lipton,⁴⁸ L. Lobo,⁴¹ A. Lobodenko,³⁸ M. Lokajicek,¹⁰ A. Lounis,¹⁸ H. J. Lubatti,⁷⁷ L. Lueking,⁴⁸ M. Lynker,⁵³ A. L. Lyon,⁴⁸ A. K. A. Maciel,⁵⁰ R. J. Madaras,⁴⁴ P. Mättig,²⁵ A. Magerkurth,⁶¹ A.-M. Magnan,¹³ N. Makovec,¹⁵ P. K. Mal,²⁸ S. Malik,⁵⁷ V. L. Malyshev,³⁴ H. S. Mao,⁶ Y. Maravin,⁴⁸ M. Martens,⁴⁸ S. E. K. Mattingly,⁷² A. A. Mayorov,³⁷ R. McCarthy,⁶⁸ R. McCroskey,⁴³ D. Meder,²³ H. L. Melanson,⁴⁸ A. Melnitchouk,⁶³ A. Mendes,¹⁴ M. Merkin,³⁶ K. W. Merritt,⁴⁸ A. Meyer,²⁰ M. Michaut,¹⁷ H. Miettinen,⁷⁵ J. Mitrevski,⁶⁶ N. Mokhov,⁴⁸ J. Molina,³ N. K. Mondal,²⁸ R. W. Moore,⁵ G. S. Muanza,¹⁹ M. Mulders,⁴⁸ Y. D. Mutaf,⁶⁸ E. Nagy,¹⁴ M. Narain,⁵⁹ N. A. Naumann,³³ H. A. Neal,⁶¹ J. P. Negret,⁷ S. Nelson,⁴⁷ P. Neustroev,³⁸ C. Noeding,²² A. Nomerotski,⁴⁸ S. F. Novaes,⁴ T. Nunnemann,²⁴ E. Nurse,⁴² V. O'Dell,⁴⁸ D. C. O'Neil,⁵ V. Oguri,³ N. Oliveira,³ N. Oshima,⁴⁸ G. J. Otero y Garzón,⁴⁹ P. Padley,⁷⁵ N. Parashar,⁵⁷ J. Park,³⁰ S. K. Park,³⁰ J. Parsons,⁶⁶ R. Partridge,⁷² N. Parua,⁶⁸ A. Patwa,⁶⁹ P. M. Perea,⁴⁶ E. Perez,¹⁷ P. Pétroff,¹⁵ M. Petteni,⁴¹ L. Phaf,³² R. Piegaia,¹ M.-A. Pleier,⁶⁷ P. L. M. Podesta-Lerma,³¹ V. M. Podstavkov,⁴⁸ Y. Pogorelov,⁵³ B. G. Pope,⁶² W. L. Prado da Silva,³ H. B. Prosper,⁴⁷ S. Protopopescu,⁶⁹ J. Qian,⁶¹ A. Quadrat,²¹ B. Quinn,⁶³ K. J. Rani,²⁸ K. Ranjan,²⁷ P. A. Rapidis,⁴⁸ P. N. Ratoff,⁴⁰ N. W. Reay,⁵⁶ S. Reucroft,⁶⁰ M. Rijssenbeek,⁶⁸ I. Ripp-Baudot,¹⁸

F. Rizatdinova,⁵⁶ C. Royon,¹⁷ P. Rubinov,⁴⁸ R. Ruchti,⁵³ V. I. Rud,³⁶ G. Sajot,¹³ A. Sánchez-Hernández,³¹ M. P. Sanders,⁴² A. Santoro,³ G. Savage,⁴⁸ L. Sawyer,⁵⁷ T. Scanlon,⁴¹ D. Schaile,²⁴ R. D. Schamberger,⁶⁸ H. Schellman,⁵¹ P. Schieferdecker,²⁴ C. Schmitt,²⁵ A. A. Schukin,³⁷ A. Schwartzman,⁶⁵ R. Schwienhorst,⁶² S. Sengupta,⁴⁷ H. Severini,⁷¹ E. Shabalina,⁴⁹ M. Shamim,⁵⁶ V. Shary,¹⁷ W. D. Shephard,⁵³ R. K. Shivpuri,²⁷ D. Shpakov,⁶⁰ R. A. Sidwell,⁵⁶ V. Simak,⁹ V. Sirotenko,⁴⁸ P. Skubic,⁷¹ P. Slattery,⁶⁷ R. P. Smith,⁴⁸ K. Smolek,⁹ G. R. Snow,⁶⁴ J. Snow,⁷⁰ S. Snyder,⁶⁹ S. Söldner-Rembold,⁴² X. Song,⁵⁰ Y. Song,⁷³ L. Sonnenschein,⁵⁹ A. Sopczak,⁴⁰ M. Sosebee,⁷³ K. Soustruznik,⁸ M. Souza,² B. Spurlock,⁷³ N. R. Stanton,⁵⁶ J. Stark,¹³ J. Steele,⁵⁷ G. Steinbrück,⁶⁶ K. Stevenson,⁵² V. Stolin,³⁵ A. Stone,⁴⁹ D. A. Stoyanova,³⁷ J. Strandberg,³⁹ M. A. Strang,⁷³ M. Strauss,⁷¹ R. Ströhmer,²⁴ D. Strom,⁵¹ M. Strovink,⁴⁴ L. Stutte,⁴⁸ S. Sumowidagdo,⁴⁷ A. Sznajder,³ M. Talby,¹⁴ P. Tamburello,⁴³ W. Taylor,⁵ P. Telford,⁴² J. Temple,⁴³ E. Thomas,¹⁴ B. Thooris,¹⁷ M. Tomoto,⁴⁸ T. Toole,⁵⁸ J. Torborg,⁵³ S. Towers,⁶⁸ T. Trefzger,²³ S. Trincaz-Duvold,¹⁶ B. Tuchming,¹⁷ C. Tully,⁶⁵ A. S. Turcot,⁶⁹ P. M. Tuts,⁶⁶ L. Uvarov,³⁸ S. Uvarov,³⁸ S. Uzunyan,⁵⁰ B. Vachon,⁵ R. Van Kooten,⁵² W. M. van Leeuwen,³² N. Varelas,⁴⁹ E. W. Varnes,⁴³ I. A. Vasilyev,³⁷ M. Vaupel,²⁵ P. Verdier,¹⁵ L. S. Vertogradov,³⁴ M. Verzocchi,⁵⁸ F. Villeneuve-Seguier,⁴¹ J.-R. Vlimant,¹⁶ E. Von Toerne,⁵⁶ M. Vreeswijk,³² T. Vu Anh,¹⁵ H. D. Wahl,⁴⁷ R. Walker,⁴¹ L. Wang,⁵⁸ Z.-M. Wang,⁶⁸ J. Warchol,⁵³ M. Warsinsky,²¹ G. Watts,⁷⁷ M. Wayne,⁵³ M. Weber,⁴⁸ H. Weerts,⁶² M. Wegner,²⁰ N. Wermes,²¹ A. White,⁷³ V. White,⁴⁸ D. Whiteson,⁴⁴ D. Wicke,⁴⁸ D. A. Wijngaarden,³³ G. W. Wilson,⁵⁵ S. J. Wimpenny,⁴⁶ J. Wittlin,⁵⁹ M. Wobisch,⁴⁸ J. Womersley,⁴⁸ D. R. Wood,⁶⁰ T. R. Wyatt,⁴² Q. Xu,⁶¹ N. Xuan,⁵³ S. Yacoob,⁵¹ R. Yamada,⁴⁸ M. Yan,⁵⁸ T. Yasuda,⁴⁸ Y. A. Yatsunenko,³⁴ Y. Yen,²⁵ K. Yip,⁶⁹ S. W. Youn,⁵¹ J. Yu,⁷³ A. Yurkewicz,⁶⁸ A. Zabi,¹⁵ A. Zatserklyaniy,⁵⁰ M. Zdrazil,⁶⁸ C. Zeitnitz,²³ D. Zhang,⁴⁸ X. Zhang,⁷¹ T. Zhao,⁷⁷ Z. Zhao,⁶¹ B. Zhou,⁶¹ J. Zhu,⁵⁸ M. Zielinski,⁶⁷ D. Ziemska,⁵² A. Zieminski,⁵² R. Zitoun,⁶⁸ V. Zutshi,⁵⁰ E. G. Zverev,³⁶ and A. Zylberstein¹⁷

(D0 Collaboration)

¹*Universidad de Buenos Aires, Buenos Aires, Argentina*²*LAFEX, Centro Brasileiro de Pesquisas Físicas, Rio de Janeiro, Brazil*³*Universidade do Estado do Rio de Janeiro, Rio de Janeiro, Brazil*⁴*Instituto de Física Teórica, Universidade Estadual Paulista, São Paulo, Brazil*⁵*University of Alberta, Edmonton, Alberta, Canada, Simon Fraser University, Burnaby, British Columbia, Canada, York University, Toronto, Ontario, Canada, and McGill University, Montreal, Quebec, Canada*⁶*Institute of High Energy Physics, Beijing, People's Republic of China*⁷*Universidad de los Andes, Bogotá, Colombia*⁸*Center for Particle Physics, Charles University, Prague, Czech Republic*⁹*Czech Technical University, Prague, Czech Republic*¹⁰*Institute of Physics, Academy of Sciences, Center for Particle Physics, Prague, Czech Republic*¹¹*Universidad San Francisco de Quito, Quito, Ecuador*¹²*Laboratoire de Physique Corpusculaire, IN2P3-CNRS, Université Blaise Pascal, Clermont-Ferrand, France*¹³*Laboratoire de Physique Subatomique et de Cosmologie, IN2P3-CNRS, Université de Grenoble 1, Grenoble, France*¹⁴*CPPM, IN2P3-CNRS, Université de la Méditerranée, Marseille, France*¹⁵*Laboratoire de l'Accélérateur Linéaire, IN2P3-CNRS, Orsay, France*¹⁶*LPNHE, IN2P3-CNRS, Universités Paris VI and VII, Paris, France*¹⁷*DAPNIA/Service de Physique des Particules, CEA, Saclay, France*¹⁸*IReS, IN2P3-CNRS, Université Louis Pasteur, Strasbourg, France, and Université de Haute Alsace, Mulhouse, France*¹⁹*Institut de Physique Nucléaire de Lyon, IN2P3-CNRS, Université Claude Bernard, Villeurbanne, France*²⁰*III. Physikalisches Institut A, RWTH Aachen, Aachen, Germany*²¹*Physikalisch-Technische Bundesanstalt, Braunschweig, Germany*²²*Physikalisch-Technische Bundesanstalt, Karlsruhe, Germany*²³*Institut für Physik, Universität Mainz, Mainz, Germany*²⁴*Ludwig-Maximilians-Universität München, München, Germany*²⁵*Fachbereich Physik, University of Wuppertal, Wuppertal, Germany*²⁶*Panjab University, Chandigarh, India*²⁷*Delhi University, Delhi, India*²⁸*Tata Institute of Fundamental Research, Mumbai, India*²⁹*University College Dublin, Dublin, Ireland*³⁰*Korea Detector Laboratory, Korea University, Seoul, Korea*³¹*CINVESTAV, Mexico City, Mexico*³²*FOM-Institute NIKHEF and University of Amsterdam/NIKHEF, Amsterdam, The Netherlands*³³*University of Nijmegen/NIKHEF, Nijmegen, The Netherlands*

- ³⁴Joint Institute for Nuclear Research, Dubna, Russia
³⁵Institute for Theoretical and Experimental Physics, Moscow, Russia
³⁶Moscow State University, Moscow, Russia
³⁷Institute for High Energy Physics, Protvino, Russia
³⁸Petersburg Nuclear Physics Institute, St. Petersburg, Russia
³⁹Lund University, Lund, Sweden, Royal Institute of Technology and Stockholm University, Stockholm, Sweden, and Uppsala University, Uppsala, Sweden
⁴⁰Lancaster University, Lancaster, United Kingdom
⁴¹Imperial College, London, United Kingdom
⁴²University of Manchester, Manchester, United Kingdom
⁴³University of Arizona, Tucson, Arizona 85721, USA
⁴⁴Lawrence Berkeley National Laboratory and University of California, Berkeley, California 94720, USA
⁴⁵California State University, Fresno, California 93740, USA
⁴⁶University of California, Riverside, California 92521, USA
⁴⁷Florida State University, Tallahassee, Florida 32306, USA
⁴⁸Fermi National Accelerator Laboratory, Batavia, Illinois 60510, USA
⁴⁹University of Illinois at Chicago, Chicago, Illinois 60607, USA
⁵⁰Northern Illinois University, DeKalb, Illinois 60115, USA
⁵¹Northwestern University, Evanston, Illinois 60208, USA
⁵²Indiana University, Bloomington, Indiana 47405, USA
⁵³University of Notre Dame, Notre Dame, Indiana 46556, USA
⁵⁴Iowa State University, Ames, Iowa 50011, USA
⁵⁵University of Kansas, Lawrence, Kansas 66045, USA
⁵⁶Kansas State University, Manhattan, Kansas 66506, USA
⁵⁷Louisiana Tech University, Ruston, Louisiana 71272, USA
⁵⁸University of Maryland, College Park, Maryland 20742, USA
⁵⁹Boston University, Boston, Massachusetts 02215, USA
⁶⁰Northeastern University, Boston, Massachusetts 02115, USA
⁶¹University of Michigan, Ann Arbor, Michigan 48109, USA
⁶²Michigan State University, East Lansing, Michigan 48824, USA
⁶³University of Mississippi, University, Mississippi 38677, USA
⁶⁴University of Nebraska, Lincoln, Nebraska 68588, USA
⁶⁵Princeton University, Princeton, New Jersey 08544, USA
⁶⁶Columbia University, New York, New York 10027, USA
⁶⁷University of Rochester, Rochester, New York 14627, USA
⁶⁸State University of New York, Stony Brook, New York 11794, USA
⁶⁹Brookhaven National Laboratory, Upton, New York 11973, USA
⁷⁰Langston University, Langston, Oklahoma 73050, USA
⁷¹University of Oklahoma, Norman, Oklahoma 73019, USA
⁷²Brown University, Providence, Rhode Island 02912, USA
⁷³University of Texas, Arlington, Texas 76019, USA
⁷⁴Southern Methodist University, Dallas, Texas 75275, USA
⁷⁵Rice University, Houston, Texas 77005, USA
⁷⁶University of Virginia, Charlottesville, Virginia 22901, USA
⁷⁷University of Washington, Seattle, Washington 98195, USA

(Received 28 November 2004; published 22 April 2005)

We search for anomalous production of heavy-flavor quark jets in association with W bosons at the Fermilab Tevatron $p\bar{p}$ Collider in final states in which the heavy-flavor quark content is enhanced by requiring at least one tagged jet in an event. Jets are tagged using one algorithm based on semileptonic decays of b/c hadrons, and another on their lifetimes. We compare $e + \text{jets}$ (164 pb^{-1}) and $\mu + \text{jets}$ (145 pb^{-1}) channels collected with the D0 detector at $\sqrt{s} = 1.96 \text{ TeV}$ to expectations from the standard model and set upper limits on anomalous production of such events.

DOI: 10.1103/PhysRevLett.94.152002

PACS numbers: 13.85.Qk, 13.85.Ni

The heavy-flavor (HF) content of jets produced in association with a W boson in $p\bar{p}$ collisions provides a test of the standard model (SM), and an excess would suggest a non-SM source of physics. The CDF Collaboration has reported such an excess in the exclusive $W + \text{jet}$ spectrum in which one jet was tagged using both

secondary-vertex tagging (SVT) and soft-lepton tagging (SLT) algorithms [1]. To check for the presence of this anomaly in our data, we too select jets tagged with both algorithms. In addition, we use benchmark SM processes to model new physics and derive upper limits on such processes.

At the Tevatron, the primary SM contributions to $W +$ HF quarks in the final state are expected from $t\bar{t}$, $Wb\bar{b}/c\bar{c}$ (where the $b\bar{b}$ or $c\bar{c}$ pairs arise from gluon splitting), and Wc final states, with additional contributions arising from single top quark or WZ (with $Z \rightarrow b\bar{b}/c\bar{c}$) production. The production of W bosons accompanied by light quarks or gluons (referred to as $W +$ jets in this Letter) contributes to the background when the light-quark or gluon jets are misidentified as jets from HF quarks. Since W bosons are identified through their $W \rightarrow e\nu$ and $W \rightarrow \mu\nu$ decays, background can arise from $Zb\bar{b}$, ZZ (with one $Z \rightarrow b\bar{b}/c\bar{c}$), and $Z +$ jets production when one of the leptons from the $Z \rightarrow \ell^+\ell^-$ decay is not detected. The main instrumental background arises from multijet processes in which a jet is misidentified as a lepton, and an imbalance in transverse momentum (\cancel{E}_T) is generated through a mismeasurement of the jets or a lepton. To be accepted, such events must also contain tagged HF jets or misidentified non-HF jets.

The data were collected with the D0 detector [2] in Run II of the Fermilab Tevatron in $p\bar{p}$ collisions at $\sqrt{s} = 1.96$ TeV. The detector components used in this analysis include the central tracker, calorimeter, and muon detectors. The central tracker consists of a silicon microstrip tracker (SMT) and a central fiber tracker (CFT), both located within a 2 T superconducting solenoidal magnet, covering the regions $|\eta| < 3.0$ and $|\eta| < 2.0$, respectively. The uranium/liquid-argon calorimeter consists of three sections, each housed in a separate cryostat [3]. The central calorimeter covers pseudorapidity $|\eta| \leq 1.1$, while the two end calorimeters extend the coverage to $|\eta| \approx 4.0$. The muon system is located outside the calorimeters and consists of layers of tracking detectors and scintillation trigger counters, one within and one beyond 1.8 T iron toroids.

The $W \rightarrow e\nu$ and $W \rightarrow \mu\nu$ candidates are selected by triggering on electrons and muons. The mean trigger efficiency for electrons with transverse momentum $p_T > 20$ GeV/c and $|\eta| < 1.1$ is $(97.0 \pm 0.3)\%$, while for muons with $p_T > 20$ GeV/c and $|\eta| < 1.6$ it is $(62.1 \pm 3.4)\%$. The integrated luminosities are 164 ± 11 pb⁻¹ for the electron and 145 ± 9 pb⁻¹ for the muon samples.

Candidates for $W \rightarrow e\nu$ are restricted by requiring just one isolated electron with $p_T > 20$ GeV/c and $|\eta| < 1.1$, defined relative to the geometrical center of the detector. Lepton isolation requires a separation in η and azimuth (ϕ) of $\mathcal{R} = \sqrt{(\Delta\eta)^2 + (\Delta\phi)^2} > 0.5$ from all jets. Electrons are defined using a cone algorithm, and by the energies deposited in calorimeter towers within a radius of $\mathcal{R} = 0.2$ of the electron axis, with at least 90% required to be within the electromagnetic portion of the calorimeter, and by the total energy in a cone of $\mathcal{R} = 0.4$ centered on the same axis, which must not exceed the electron's energy by more than 15%. In addition, the shower shape must be compatible with that expected for an electron.

Candidates for $W \rightarrow \mu\nu$ must contain just one isolated muon with $p_T > 20$ GeV/c and $|\eta| < 1.6$, defined relative

to the geometrical center of the detector. Muons must satisfy two additional isolation criteria: (i) the transverse energy deposited in the calorimeter in the annular region of $0.1 < \mathcal{R} < 0.4$ around the muon's path must be smaller than 2.5 GeV and (ii) the vector sum of the p_T of all tracks within $\mathcal{R} = 0.5$ of the muon's trajectory must be less than 2.5 GeV/c (excluding the track matched to the muon).

Lepton identification is refined by requiring the trajectory of a track reconstructed in the SMT and CFT to match either the position of the electron energy cluster in the calorimeter or the position of hits in the muon detector. To complete the selection, all events are also required to have $\cancel{E}_T > 20$ GeV, and the azimuthal angle between the lepton and the direction of the \cancel{E}_T must be greater than 22.5°. To eliminate poorly reconstructed events, the primary vertex (PV) of the event must contain at least three tracks, and its z position (along the beam) has to be closer than 60 cm from the center of the detector. Finally, to reject a multijet background, the reconstructed transverse mass of (ℓ, \cancel{E}_T) must be consistent with that of the W boson, $40 < M_{W_T} < 120$ GeV/c² (i.e., we assume that \cancel{E}_T corresponds to the transverse energy of the neutrino).

After selecting W -boson candidates, we evaluate the HF-quark content of each event. Jets are defined using an iterative seed-based cone algorithm, clustering calorimeter energy within $\mathcal{R} = 0.5$ [4]. This is subsequently corrected for the jet energy scale (JES), based on momentum balance in photon + jet events. We consider only jets with $E_T > 25$ GeV and $|\eta| < 2.5$ and evaluate them using two HF-tagging algorithms, as described below.

The soft-lepton tagging algorithm is based on low- p_T muons that arise from semileptonic decays of HF quarks produced in a jet nearby in (η, ϕ) . Only muons with $p_T > 4$ GeV/c and $|\eta| < 2.0$ are considered. To reject a $Z \rightarrow \mu\mu$ background, we require $p_T < 15$ GeV/c for the muon. Jets with a muon within $\mathcal{R} = 0.5$ of the jet axis are deemed tagged. Typical SLT efficiencies for b -quark jets are $\approx 11\%$, 3% for c -quark jets, and 0.4% for light-quark jets. The muon present in SLT events enhances the average single-muon trigger efficiency from $(62.1 \pm 3.4)\%$ to $(68.4 \pm 3.5)\%$.

Secondary-vertex tagging is used to identify displaced secondary vertices (SV) of long-lived particles. To form these SV, charged tracks are selected on the basis of the significance of their distance-of-closest-approach (dca) to the PV. Tracks are first grouped in $\mathcal{R} = 0.5$ cones around a seed track with $p_T > 1$ GeV/c and $dca/\sigma_{dca} > 3.5$, where σ_{dca} is the uncertainty on the track's dca. Protovertices are formed by adding tracks to the initial grouping, provided their contribution to the χ^2 of the vertex fit is small. Secondary vertices are selected by requiring the transverse distance from the SV to the beam direction, L_{xy} , to be less than 2.6 cm, and the decay-length significance, $\frac{L_{xy}}{\sigma_{L_{xy}}}$, to be greater than 7, where $\sigma_{L_{xy}}$ is the estimated uncertainty on L_{xy} calculated from the error matrices of the tracks in the vertex. Jets are considered tagged by this algorithm when a

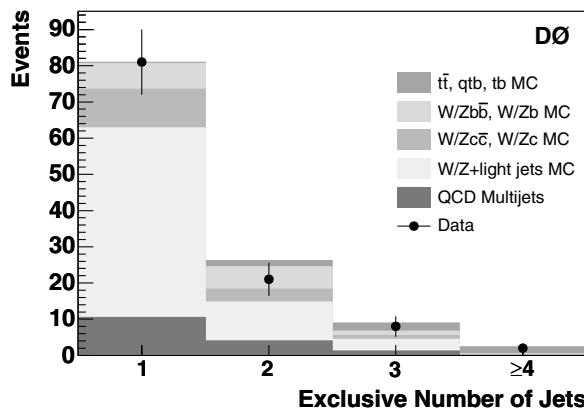


FIG. 1. Exclusive jet multiplicity for W -boson candidate events with at least one SLT-tagged jet. The fourth bin represents the sum of events containing four or more jets.

SV lies within $\mathcal{R} = 0.5$ of the jet axis. This SVT algorithm exhibits a typical tagging rate for b -quark jets of $\approx 25\%$, 8% for c -quark jets, and 0.25% for light-quark jets.

To predict SM rates, Monte Carlo (MC) events are generated for the processes mentioned above, with the exception of multijet production, which is estimated from data (see below). $W/Z +$ jets (both HF and light-quark jets), $t\bar{t}$, and diboson processes are simulated with ALPGEN [5]. Single top-quark processes are simulated using COMPHEP [6]. All events are generated with $m_{top} = 175 \text{ GeV}/c^2$. Hadronization and showering of these events is based on PYTHIA [7]. The exceptions are $W/Z + b$ processes, where Zb is simulated using PYTHIA, and the contribution from Wb is estimated from the parametrized MCFM MC [8] and used to calculate a cross section relative to $Wb\bar{b}$ production assuming the jet- p_T spectrum from PYTHIA for inclusive W boson production. All MC events are generated at $\sqrt{s} = 1.96 \text{ TeV}$, using CTEQ5L [9] parton distribution functions and a detailed detector simulation based on GEANT [10]. To simulate the effect of multiple interactions in beam crossings, a Poisson-distributed minimum-bias event overlay, with an average of 0.8 events, is included for all events. To avoid an incorrect combination of cross sections among simulated $W/Z +$ jets samples, only events with the same number of reconstructed jets as the number of initial partons are retained. The background from multijet events, in which a jet is misidentified as a lepton, is evaluated using the “matrix method” as follows. Defining a “tight” $W +$ jets candidate sample that has the lepton-identification criteria described above, and a “loose” sample in which some of these identification criteria are relaxed, a comparison of the probabilities for true leptons to be identified as loose and jets as tight leptons (as determined from independent studies of samples of pure leptons and pure jets) yields the fractions of true leptons and of misidentified jets in the tight and loose samples.

After the W -boson and jet selections, we apply the two HF-tagging algorithms to the jets. The MC samples are

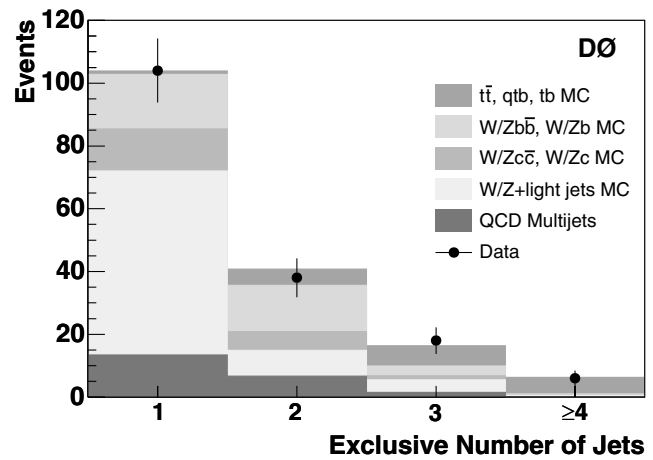


FIG. 2. Exclusive jet multiplicity for W -boson candidate events with at least one SVT-tagged jet. The fourth bin represents the sum of events containing four or more jets.

normalized to the appropriate luminosity and corrected for differences in HF-tagging and lepton-identification efficiencies relative to data. Also, data collection inefficiencies from trigger requirements are introduced into the simulated samples based on independent data measurements for each set of selections.

In the following, we combine the $e +$ jets and $\mu +$ jets samples, and Figs. 1 and 2 show the exclusive number of jets in events with at least one SLT-tagged jet and at least one SVT-tagged jet, respectively. The transverse mass for W -boson candidates containing at least one SLT- or one SVT-tagged jet, shown in Fig. 3, agrees well with SM expectation. The distribution for events with at least one jet tagged with both algorithms is shown in Fig. 4.

The dominant sources of experimental uncertainty are as follows: (i) a 6.5% uncertainty on integrated luminosity, (ii) a 6% per jet uncertainty from JES corrections and jet identification, (iii) a 10% per jet uncertainty from the HF-tagging algorithms, and (iv) a $10\%-18\%$ uncertainty on the predicted MC cross sections (depending on the

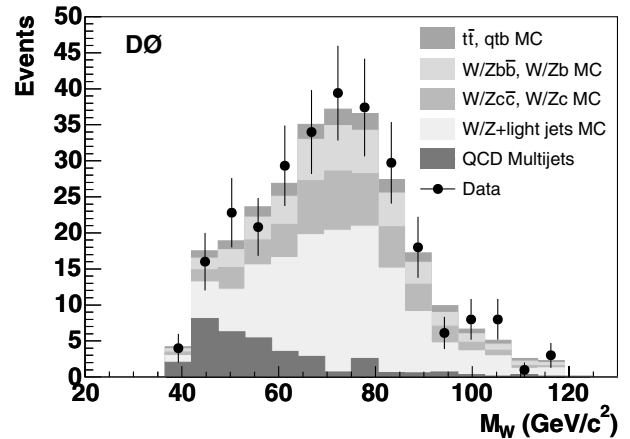


FIG. 3. Transverse W -boson mass for events containing at least one SLT- or one SVT-tagged jet.

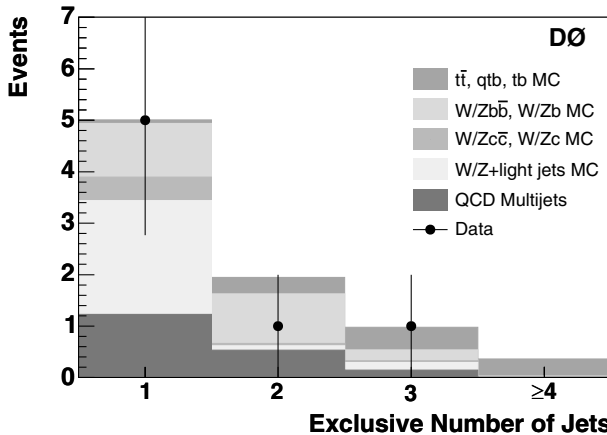


FIG. 4. Exclusive jet multiplicity of W -boson candidate events with at least one jet tagged with both the SVT and SLT algorithms. The fourth bin represents the sum of events containing four or more jets.

sample). The total systematic uncertainties on $t\bar{t}$, single top-quark, and $W/Z + \text{jets}$ backgrounds are 16%, 21%, and 22%, respectively.

No excess is observed in the “doubly-tagged” jet sample. We therefore set a limit on the rate of anomalous HF-quark production in association with a W boson. Because we do not propose a model for such production, we do not base this limit on any specific efficiency or jet spectrum. We quote limits on the number of events beyond SM expectation per exclusive jet bin. The 95% confidence level (C.L.) upper limits for additional event production in each bin are shown in Table I. These limits are calculated using a modified Frequentist (CL_s) method [11].

Assuming that anomalous HF production has the same event topology as certain SM processes, the above limits can be translated into limits on cross sections. To this end, we consider two benchmark scenarios:

(1) “ $Wb\bar{b}$ -like” production in which two b quarks are produced in association with a W boson. In this scenario, additional light quarks or gluons can be produced and thereby shift the event topology to more than two jets. Jets not within the acceptance of the detector can also cause the event topology to drop to less than two jets. We model this production using efficiencies for SM $W/Z + b\bar{b}$ production.

(2) “Toplike” production in which a heavy particle is produced and decays to a W boson and a b quark. An event can contain two such heavy particles (“ $t\bar{t}$ -like”) or one

TABLE II. Cross-section upper limits in pb, based on the hypotheses of $Wb\bar{b}$ -like and toplike anomalous production of exclusive jets. Each value must still be corrected for the efficiency of reconstructing the predicted number of jets.

Model	1 jet	2 jets	3 jets	≥ 4 jets
$Wb\bar{b}$ -like	35.0	9.2	6.0	4.5
Toplike	12.6	8.0	11.3	15.4

heavy quark (“single-top-like”), with additional light or heavy quarks and gluons possible for both cases. We model this scenario using the combined cross-section weighted efficiencies for SM $t\bar{t}$ and single top-quark production.

To calculate a limit on exclusive jet production for each case, we first ignore the probability for reconstructing the predicted number of jets, providing a model-independent comparison of processes with specific jet topologies. The remaining efficiency represents the effect of W -boson selection and HF tagging, and limits for specific models can be extracted by multiplying this value by the efficiency to reconstruct the number of jets in each exclusive jet bin. This is given in Table II.

To evaluate an upper cross-section limit on inclusive jet production for each scenario, we reintroduce the efficiency for reconstructing the predicted jets and sum the relevant exclusive jet bins as shown in Table III. For inclusive $Wb\bar{b}$ -like anomalous production, the contribution from higher bins being negligible, we sum the first two $W + \text{jets}$ bins. For toplike anomalous production, we sum all $W + \text{jets}$ bins, except $n = 1$, where the contribution is again negligible. Table III shows the 95% C.L. event limits for the combinations of bins for these two hypotheses, and also the corresponding anomalous HF production limits. The jet reconstruction efficiency is included in the calculations, and the limits contain the expected efficiencies for the specified SM processes.

In summary, we observe no excess beyond the SM prediction for heavy-flavor quark production in association with W bosons in 164 pb^{-1} of data in $e + \text{jets}$ and 145 pb^{-1} in $\mu + \text{jets}$ channels. Using a sample of events containing at least one jet tagged with both the SLT and SVT algorithms, we derive 95% C.L. limits on anomalous heavy-flavor production (Table I). Using benchmark SM processes, we also derive limits of 26.4 pb for $Wb\bar{b}$ -like and 14.9 pb for toplike anomalous scenarios. For comparison, the D0 Collaboration has published a similar study in

TABLE I. The numbers of observed and predicted W -boson events with at least one jet tagged by both the SLT and SVT algorithms, as a function of exclusive jet multiplicity. Also shown are the 95% C.L. limits in the form of additional events.

Source	1 jet	2 jets	3 jets	≥ 4 jets
Data observation	5	1	1	0
SM prediction	5.0 ± 1.2	2.0 ± 0.5	1.0 ± 0.2	0.4 ± 0.1
95% C.L. limit (excess events)	6.7	3.9	4.1	3.0

TABLE III. 95% C.L. limits for the number of events summed over the indicated jet bins. Also shown are cross-section limits based on the hypotheses of $Wb\bar{b}$ -like and toplike anomalous production for the selected number of jets.

Source	1,2 jets	≥ 2 jets
Data observation	6	2
SM prediction	6.9 ± 1.2	3.3 ± 0.5
95% C.L. limit (events)	6.6	4.4
Model		
$Wb\bar{b}$ -like	26.4 pb	...
Toplike	...	14.9 pb

the form of a search for $Wb\bar{b}$ production [12]. Based on the two-jet topology, with both jets HF tagged, that study sets a 95% C.L. upper cross-section limit of 6.6 pb on $Wb\bar{b}$ production for jets with $p_T > 20$ GeV/ c and $\mathcal{R}(b, \bar{b}) > 0.75$.

We thank the staffs at Fermilab and collaborating institutions and acknowledge support from the Department of Energy and National Science Foundation (USA), Commissariat à l'Energie Atomique and CNRS/Institut National de Physique Nucléaire et de Physique des Particules (France), Ministry of Education and Science, Agency for Atomic Energy and RF President Grants Program (Russia), CAPES, CNPq, FAPERJ, FAPESP, and FUNDUNESP (Brazil), Departments of Atomic Energy and Science and Technology (India), Colciencias (Colombia), CONACyT (Mexico), KRF (Korea), CONICET and UBACyT (Argentina), The Foundation for Fundamental Research on Matter (The Netherlands), PPARC (United Kingdom), Ministry of Education (Czech Republic), Canada Research Chairs Program, CFI, Natural

Sciences and Engineering Research Council and WestGrid Project (Canada), BMBF and DFG (Germany), A. P. Sloan Foundation, Research Corporation, Texas Advanced Research Program, and the Alexander von Humboldt Foundation.

*Visitor from University of Zurich, Zurich, Switzerland.

- [1] CDF Collaboration, D. Acosta *et al.*, Phys. Rev. D **65**, 052007 (2002).
- [2] D0 Collaboration, V. Abazov *et al.* (to be published); T. LeCompte and H. T. Diehl, Annu. Rev. Nucl. Part. Sci. **50**, 71 (2000).
- [3] D0 Collaboration, S. Abachi *et al.*, Nucl. Instrum. Methods Phys. Res., Sect. A **338**, 185 (1994).
- [4] G. C. Blazey *et al.*, in *Proceedings of the Workshop “QCD and Weak Boson Physics in Run II,”* edited by U. Baur, R. K. Ellis, and D. Zeppenfeld (Fermilab Report No. Fermilab-Pub-00/297, 2000), p. 47.
- [5] M. L. Mangano, M. Moretti, F. Piccinini, R. Pittau, and A. Polosa, J. High Energy Phys. 07 (2003) 001.
- [6] A. Pukhov *et al.*, hep-ph/9908288.
- [7] T. Sjöstrand *et al.*, Comput. Phys. Commun. **135**, 238 (2001).
- [8] J. Campbell and R. K. Ellis, Phys. Rev. D **65**, 113007 (2002), <http://mcfm.fnal.gov>.
- [9] CTEQ Collaboration, H. L. Lai *et al.*, Eur. Phys. J. C **12**, 375 (2000).
- [10] R. Brun and F. Carminati, computer code, CERN Program Library Long Writeup w5013, CERN, 1993.
- [11] T. Junk, Nucl. Instrum. Methods Phys. Res., Sect. A **434**, 435 (1999); A. Read, in “1st Workshop on Confidence Limits,” CERN Report No. CERN-2000-005, 2000.
- [12] D0 Collaboration, V. Abazov *et al.*, Phys. Rev. Lett. **94**, 091802 (2005).